We thank Peter Köhler for his useful comment and advices.

Accordingly, we have modifed section 2 and figure 2 in the revised manuscript. Particularly:
- we now recommend using the final spline-smoothed GHG data published in Köhler et al. (2017).
- regarding the issue related to missing N_2O data before 134 ka we also follow his suggestion to linearly increase N_2O from 201 ppb at 140 ka to 218.74 ppb at 134.5 ka.
- regarding the greenhouse gas concentration values to use for the 140 ka spin-up, we now recommend using the averaged CO_2 and CH_4 concentrations between 139 and 141 ka, i.e. 191 ppm and 385 ppm respectively. Consequently, the CO_2 and CH_4 values between 140 and 139 ka will be linearly interpolated between the 140 ka spin-up values and the values at 139 ka from the spline-smoothed curves to avoid artificial jumps: 196.68 ppm and 287.65 ppb respectively.

Please find attached below the revised section 2 and Figure 2.

Many thanks again.

Reference:

Köhler, P., Nehrbass-Ahles, C., Schmitt, J., Stocker, T. F., and Fischer, H.: A 156 kyr smoothed history of the atmospheric greenhouse gases CO2, CH4 and N2O and their radiative forcing, Earth Syst. Sci. Data, 9, 363-387, https://doi.org/10.5194/essd-9-363-2017, 2017

GHG records are available solely from Antarctic ice cores across the time interval 140-127 ka (Fig. 2). LIG GHG records from the NEEM and other Greenland ice cores are affected by stratigraphic disturbances and in-situ CO_2, CH_4 and N_2O production (e.g. Tschumi and Stauffer, 2000; NEEM community members, 2013). The NGRIP ice core provides a continuous and reliable CH_4 record but it only extends back to ∼123 ka (North Greenland Ice Core Project members, 2004). After a brief description of existing atmospheric CO_2, CH_4 and N_2O records (below), we recommend using recent spline-smoothed GHG curves calculated from a selection of those records (Köhler et al., 2017). They have the benefit to provide continuous GHG records, with a temporal resolution of 1 yr on the commonly-used AICC2012 gas age scale (Bazin et al., 2013; Veres et al., 2013). Note that this time scale is associated with an average 1σ absolute error of ∼2 kyr between 140 and 127 ka.

Atmospheric CO_2 concentrations have been measured on the EDC and TALDICE ice cores (Fig. 2). The EDC records from Lourantou et al. (2010) and Schneider et al. (2013) agree well overall. The Schneider et al. (2013) dataset depicts a long-term CO_2 increase starting at ∼137.8 ka and ending at ∼128.5 ka with a centennial-scale CO_2 rise above the subsequent LIG CO_2 values, also referred to as an "overshoot". The CO_2 overshoot is smaller in the Schneider et al. (2013) dataset compared to a similar feature measured in Lourantou et al. (2010): while the former displays a relatively constant CO_2 concentration of ∼275 ppm between 128 and 126 ka, the latter shows a CO_2 decrease from 280 to 265 ppm between 128 and 126 ka. The offsets between CO_2 records from the same EDC core are likely related to the different air extraction techniques used in the two studies (Schneider et al., 2013). The smoothed spline CO_2 curve across TII we recommend using as forcing is based on those two EDC dataset and the calculation method accounts for such potential difference in local maxima (details provided in Köhler et al. (2017)).

Atmospheric CH_4 concentration records from Vostok, EDML, EDC and TALDICE agree well within the gas-age uncertainties attached to each core (Fig. 2). They illustrate a slow rise from ∼390 to 540 ppb between ∼137 ka and 129 ka that is followed by an abrupt increase of ∼200 ppb reaching maximum LIG values at ∼128.5 ka. Because CH_4 sources are located mostly in the NH, an interpolar concentration difference (IPD) between Greenland and Antarctic CH_4 records exists.

For instance, an IPD of ∼14 ppb, ∼34 ppb and ∼43 ppb is reported during the LGM, Heinrich Stadial 1 and the Bølling warming respectively (Baumgartner et al., 2012). However, without reliable CH_4 records from Greenland ice cores, it remains challenging to estimate the evolution of the IPD across TII. Hence, for the atmospheric CH_4 forcing of future TII transient simulations, we recommend using the smoothed spline CH_4 curve which is solely based on the EDC CH_4 record (Köhler et al., 2017), recognising that the values may be 1-4% lower than the actual global average.

Both CO_2 and CH_4 concentrations undergo some rapid changes around 140 ka, which is also the time when the models should spin up. To avoid possible artificial abrupt changes in the GHG we recommend using as spin-up CO_2 and CH_4 concentrations, the average values obtained for the interval 139-141 (i.e. 191 ppm for CO_2 and 385 ppb for CH_4, Table 1). Consequently, CO_2 and CH_4 changes between 140 and 139 ka provided in the forcing scenarios are linearly interpolated between the 140 ka spin-up values and those at 139 ka of 196.68 ppm for CO_2 and 287.65 ppb for CH_4. From 139 ka, the use of the spline-smoothed curves from Köhler et al. (2017) are recommended.

Atmospheric TALDICE, EDML and EDC N_2O records are available between 134.5 and 127 ka (Fig. 2) (Schilt et al., 2010; Flückiger et al., 2002). From 134.5 to 128 ka, N_2O levels increase from ∼220 to 270 ppb. Following a short decrease until ∼127 ka, N_2O concentrations stabilise afterwards. No reliable atmospheric N_2O concentrations are available beyond 134 ka as N_2O concentrations measured in the air trapped in ice from the penultimate glacial maximum are affected by in-situ production related to microbial activity (Schilt et al., 2010). During the LGM (considered here as the time interval 26-21 ka), the average N_2O level was ∼201 ppb. Assuming the LGM is an analogue for the penultimate glacial maximum, we propose a 140 ka spin-up value and N_2O transient forcing curve that starts with a 201 ppb level and then linearly increases to 218.74 ppb at 134.5 ka. From 134.5 ka, we recommend using the N_2O smoothed spline curve calculated by Köhler et al. (2017) and which is based on the TALDICE and EDC discrete N_2O measurements.

Note that the CO_2 and N_2O levels from the spline curves at 127 ka (274 ppm and 257 ppb) only differ from the values chosen as boundary conditions for the PMIP4 *lig127k* equilibrium experiment by 1 ppm and 2 ppb respectively (Otto-Bliesner et al., 2017; Köhler et al., 2017). The comparison is less direct for CH_4. Indeed a global CH_4 value (685 ppm) rather than an Antarctic ice core-based CH_4 value (e.g. CH_4 level of 660 ppm at 127 ka in Köhler et al. (2017)) is proposed as forcing for the *lig127k* simulations. However, this difference in global atmospheric CH_4 and Antarctic ice core CH_4 concentration is similar to the one observed during the mid-Holocene (23 ppb) (Otto-Bliesner et al., 2017; Köhler et al., 2017).

References

Baumgartner, M., Schilt, A., Eicher, O., Schmitt, J., Schwander, J., Spahni, R., Fischer, H., and Stocker, T. F.: High-resolution interpolar difference of atmospheric methane around the Last Glacial Maximum, Biogeosciences, 9, 3961–3977, https://doi.org/10.5194/bg-9-3961-2012, https://www.biogeosciences.net/9/3961/2012/, 2012.

Bazin, L., Landais, A., Lemieux-Dudon, B., Kele, H. T. M., Veres, D., Parrenin, F., Martinerie, P., Ritz, C., Capron, E., Lipenkov, V., Loutre, M.-F., Raynaud, D., Vinther, B., Svensson, A., Rasmussen, S. O., Severi, M., Blunier, T., Leuenberger, M., Fischer, H., Masson-Delmotte, V., Chappellaz, J., and Wolff, E.: An optimized multi-proxy, multi-site Antarctic ice and gas orbital chronology (AICC2012): 120-800 ka, Climate of the Past, 9, 1715–1731, 2013.

Flückiger, J., Monnin, E., Stauffer, B., Schwander, J., Stocker, T., Chappellaz, J., Raynaud, D., and Barnola, J.-M.: High-resolution Holocene N_2O ice core record and its relationship with CH_4 and CO_2, Global Biogeochemical Cycles, 16, 10–1–10–8, https://doi.org/10.1029/2001GB001417, 2002.

Köhler, P., Nehrbass-Ahles, C., Schmitt, J., Stocker, T., and Fischer, H.: A 156 kyr smoothed history of the atmospheric greenhouse gases CO_2, CH_4, and N_2O and their radiative forcing, Earth System Science Data, 9, 363–387, https://doi.org/10.5194/essd-9-363-2017, 2017.

Lourantou, A., Lavric, J., Kohler, P., Barnola, J.-M., Paillard, D., Michel, E., Raynaud, D., and Chappellaz, J.: Constraint of the CO_2 rise by new atmospheric carbon isotopic measurements during the last deglaciation, Global Biogeochemical Cycles, 24, doi:10.1029/2009GB003 545, 2010.

NEEM community members: Eemian interglacial reconstructed from a Greenland folded ice core, Nature, 493, 489–494, https://doi.org/doi:10.1038/nature11789, 2013.

North Greenland Ice Core Project members: High-resolution record of Northern Hemisphere climate extending into the last interglacial period, Nature, 431, 147–151, 2004.

Otto-Bliesner, B., Braconnot, P., Harrison, S., Lunt, D., Abe-Ouchi, A., Albani, S., Bartlein, P., Capron, E., Carlson, A., Dutton, A., Fischer, H., Goelzer, H., Govin, A., Haywood, A., Joos, F., Legrande, A., Lipscomb, W., Lohmann, G., Mahowald, N., Nehrbass-Ahles, C., Peterschmitt, J.-Y., Pausata, F.-R., Peterschmitt, J.-Y., Phipps, S., Renssen, H., and Zhang, Q.: The PMIP4 contribution to CMIP6 - Part 2: Two Interglacials, scientific objectives and experimental design for Holocene and Last Interglacial simulations, Geoscientific Model Development, pp. 3979 – 4003, https://doi.org/10.5194/gmd-10-3979-2017, 2017.

Schilt, A., Baumgartner, M., Blunier, T., Schwander, J., Spahni, R., Fischer, H., and Stocker, T.: Glacial-interglacial and millennial-scale variations in the atmospheric nitrous oxide concentration during the last 800,000 years, Quaternary Science Reviews, 29, 182–192, https://doi.org/10.1016/j.quascirev.2009.03.011, 2010.

Schneider, R., Schmitt, J., Köhler, P., Joos, F., and Fischer, H.: A reconstruction of atmospheric carbon dioxide and its stable carbon isotopic composition from the penultimate glacial maximum to the last glacial inception, Climate of the Past, 9, https://doi.org/10.5194/cp-9-2507-2013, 2013.

Tschumi, J. and Stauffer, B.: Reconstructing past atmospheric CO_2 concentration based on ice-core analyses: open questions due to in situ production of CO_2 in the ice, Journal of Glaciology, 46, 45–53, 2000.

Veres, D., Bazin, L., Landais, A., Kele, H. T. M., Lemieux-Dudon, B., Parrenin, F., Martinerie, P., Blayo, E., Blunier, T., Capron, E., Chappellaz, J., Rasmussen, S. O., Severi, M., Svensson, A., Vinther, B., and Wolff, E.: The Antarctic ice core chronology (AICC2012): an optimized multi-parameter and multi-site dating approach for the last 120 thousand years, Climate of the Past, 9, 1733–1748, 2013.

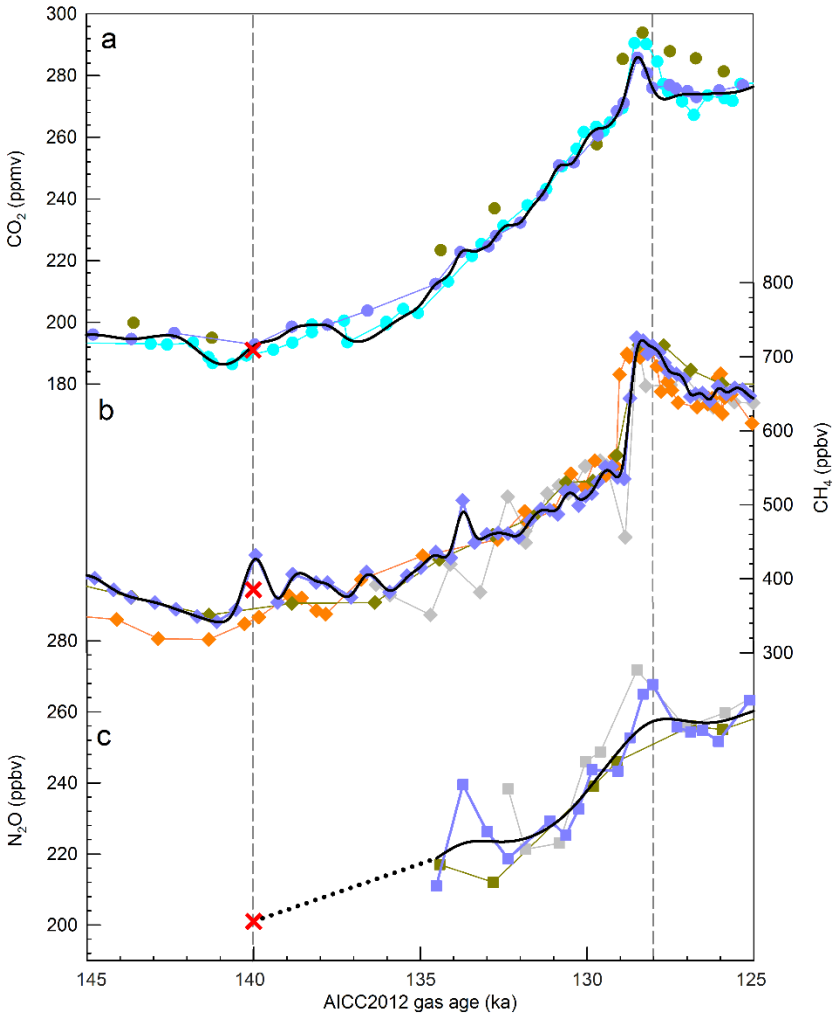

Figure 2. Atmospheric greenhouse gas concentrations: Atmospheric trace gases through the penultimate deglaciation from Antarctic ice cores displayed on the AICC2012 chronology (Bazin et al., 2013; Veres et al., 2013). a) Atmospheric CO_2 concentrations from EDC (turquoise and blue) (Lourantou et al., 2010; Schneider et al., 2013) and TALDICE (green) (Schneider et al., 2013). b) Atmospheric CH4 concentration from EDC (Loulergue et al., 2008) (blue), Vostok (Petit et al., 1999) (orange), TALDICE (Buiron et al., 2011) (green) and EDML (Capron et al., 2010) (grey). c) Atmospheric N_2O concentration from EDC (Flückiger et al., 2002) (blue), EDML (Schilt et al., 2010) (grey) and TALDICE (Schilt et al., 2010) (green). Transient experiments should be forced by the smoothed splines of CO_2, CH_4 and N_2O concentrations as shown in black (Köhler et al, 2017). Between 140 ka and 134.5 ka, N_2O should increase linearly from 201 ppb to 218.74 ppb at (dashed black line). Red crosses indicate the 140 ka spin-up values for CO_2, CH_4 and N_2O concentrations (191 ppm, 385 ppb and 201 ppb, respectively).